Multifunctional supercapacitor based on 2D nanosheets on flexible carbon nanotube film

Qiufan Wang[a], Xiao Liang[a], Daohong Zhang[a*], Menghe Miao[b*]

[a] Key Laboratory of Catalysis and Energy Materials Chemistry of Ministry of Education & Hubei Key Laboratory of Catalysis and Materials Science, Hubei R&D Center of Hyperbranched Polymers Synthesis and Applicatoins, South-Central University for Nationalities, Wuhan 430074, China.

[b] CSIRO Manufacturing, 75 Pigdons Road, Waurn Ponds, Victoria 3216, Australia

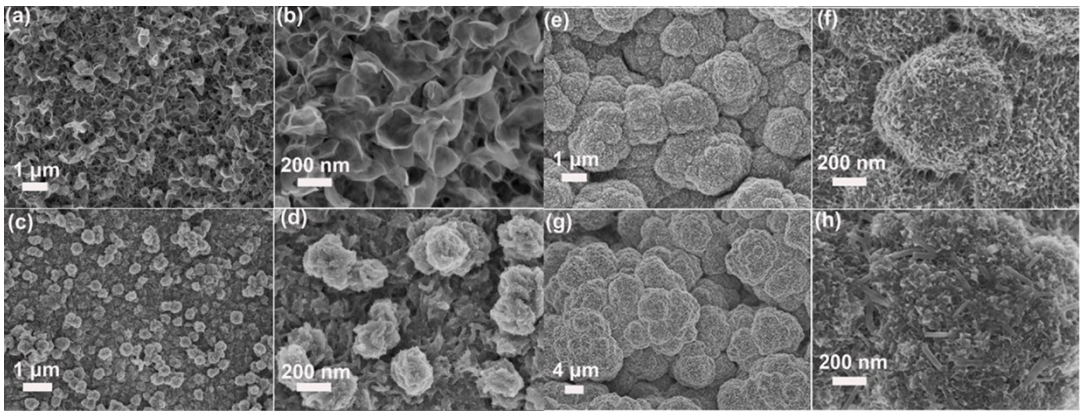

Figure S1. SEM images: (a-b) MoS_2/CNT; (c-d) MoS_2/PEDOT/CNT-2; (e-f) MoS_2/PEDOT/CNT-180; (g-h) MoS_2/PEDOT/CNT-240.

The MoS_2 samples are composed of nanosheets arranged randomly on the CNT film (Figure S1a-b). The SEM images of the MoS_2/PEDOT/CNT-2 are displayed in Figure S1c-d, which demonstrate pleated globules of PEDOT with diameters of ~200 nm coated on MoS_2/CNT. With the deposition time increasing to 180 min, the MoS_2/CNT was fully covered by PEDOT globules with larger size of ~700 nm (Figure S1e-f). The accumulation of globules are accumulated and growing larger when electrodeposition time was increased to 240 min (Figure S1g-h).

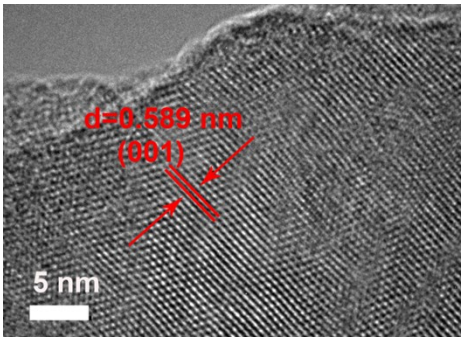

Figure S2. High-resolution TEM (HRTEM) image of SnS_2 nanosheets.

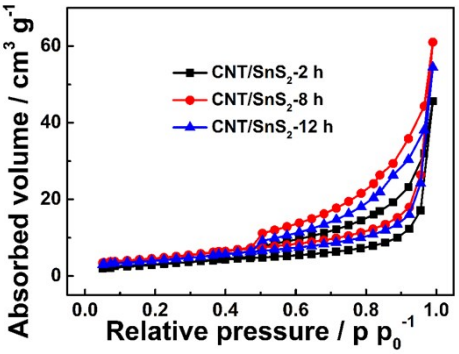

Figure S3. Nitrogen adsorption-desorption isotherms of SnS_2 sample.

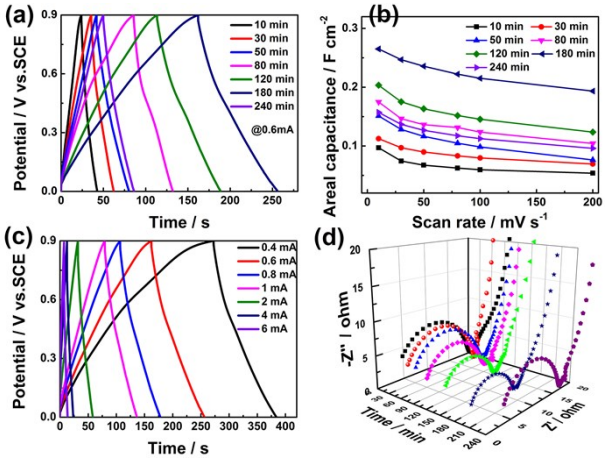

Figure S4. Electrochemical properties of MoS_2/PEDOT/CNT electrodes. (a) GCD curves of MoS_2/PEDOT/CNT-*n* electrodes at 0.6 mA, (b) capacitance of the MoS_2/PEDOT/CNT-*n* electrodes at different scan rates, (c) GCD curves of MoS_2/PEDOT/CNT-180 electrodes, (d) EIS curves of MoS_2/PEDOT/CNT-*n* electrodes.

Specific capacitances calculated from the CV curves at various scan rates are shown in Figure S4b, where the capacitance increased significantly with increasing deposition time from 10 to 180 min, and PEDOT globules became thicker and form a cross-linking network structure, which is conducive to ion transport. However, when

the electrodeposition time was increased to 240 min, the PEDOT globules became thick particles, which limit ion access to the inner surface area for electrochemical charge storage and thus lead the areal capacitance. GCD curves of the MoS_2/PEDOT/CNT under different currents (Figure S4c) exhibit nearly symmetrical triangle curves for charging and discharging process. The EIS curves of the MoS_2/PEDOT/CNT-n electrodes are depicted in Figure S4d. All the Nyquist plots are composed of two parts, a semicircle in the high frequency region and a straight slope in the low frequency region. The diameter of the semicircle is often considered to be related to the charge-transfer resistance (R_{ct}) of the electrode whereas the slope of the straight line represents ion diffusion from the electrolyte solution to the electrode interface. The R_{ct} of the MoS_2/PEDOT/CNT-180 electrode is the smallest, providing the fastest charge transport.

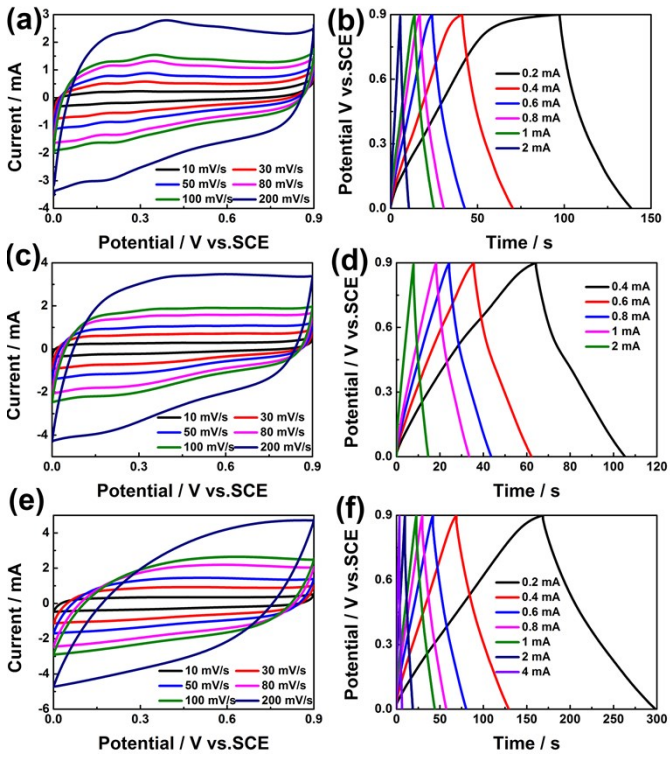

Figure S5. Electrochemical properties of the MoS_2/PEDOT/CNT: (a-b) MoS_2/PEDOT/CNT-10; (e-f) MoS_2/PEDOT/CNT-30; (g-h) MoS_2/PEDOT/CNT-50.

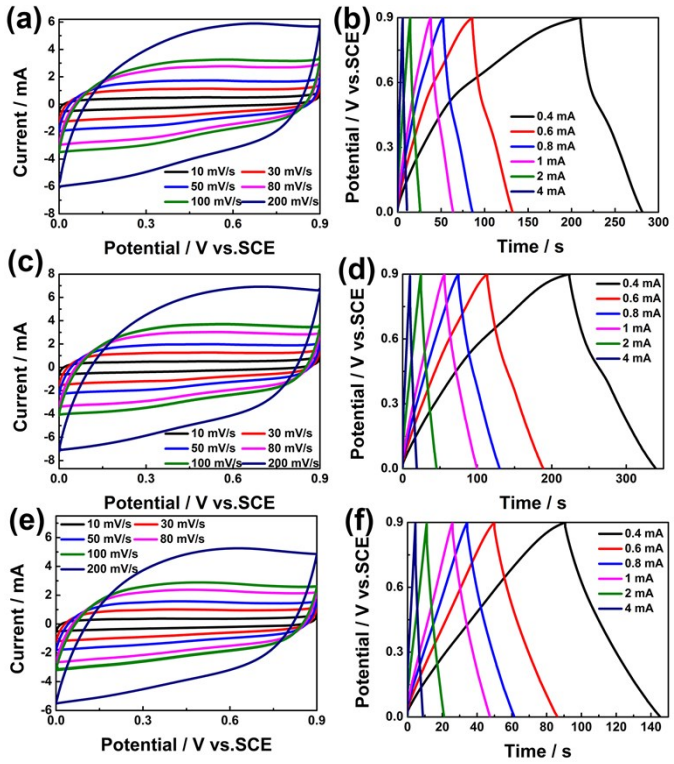

Figure S6. Electrochemical properties of the MoS_2/PEDOT/CNT: (a-b) MoS_2/PEDOT/CNT-80; (e-f) MoS_2/PEDOT/CNT-120; (g-h) MoS_2/PEDOT/CNT-240.

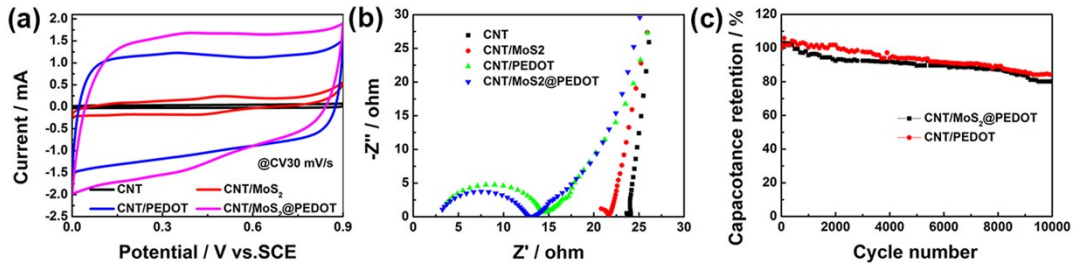

Figure S7. Electrochemical performances of pure CNT, MoS_2/CNT, PEDOT/CNT and MoS_2/PEDOT/CNT electrodes in a three-electrode system: (a) CV curves, (b) EIS curves and (c) Cycling performance.

The CV curves of the CNT, MoS_2/CNT, PEDOT/CNT and MoS_2/PEDOT/CNT-180 composite electrodes at 30 mV s^{-1} are illustrated in Figure S7a. The MoS_2/PEDOT/CNT exhibited significantly higher current response than CNT, MoS_2/CNT and PEDOT/CNT, indicating a much higher capacitance to deliver. This result may be explained with the aid of Figure S7b. The equivalent series resistances (ESRs) of CNT, MoS_2/CNT, PEDOT/CNT and MoS_2/PEDOT/CNT obtained from the intersection point of the curves with the axis of real impedance are 24.05 Ω, 21.61

Ω, 14.46 Ω and 13.21 Ω, respectively. The difference in ESR of the electrodes can be attributed to their different conductivities. As shown in Figure S8c, ESR of the MoS_2/PEDOT/CNT composite is much lower than the CNT, MoS_2/CNT and PEDOT/CNT. The good conductivity of the material may be due to the intimate contact between the CNT, MoS_2 and PEDOT. Although PEDOT possesses controllable conductivity and high electrochemical activity, a pure PEDOT electrode suffers from poor cycling stability because the redox sites in the polymer backbone are not sufficiently stable. The backbone of the polymer can be destroyed within a rather limited number of charge/discharge cycles. The cyclic stabilities of the PEDOT/CNT and MoS_2/PEDOT/CNT electrodes examined by GCD tests for 10,000 cycles using a three-electrode system are shown in Figure S7c. The specific capacitance of PEDOT/CNT and MoS_2/PEDOT/CNT electrodes maintained at 80.1% and 84.6% after 10000 cycles, respectively. This result highlights that the CNT film and MoS_2 materials improved the stability of the MoS_2/PEDOT/CNT electrode, which provides long cycle life and high rate capability.

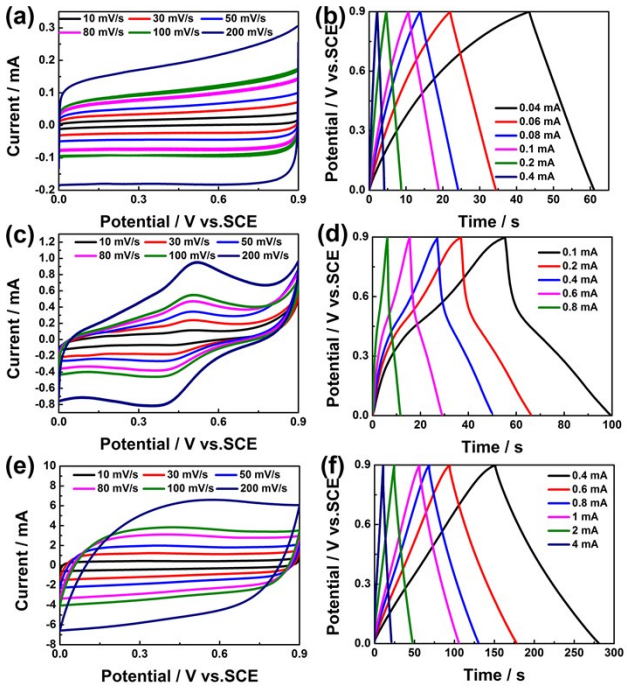

Figure S8. Electrochemical properties of the CNT(a-b), MoS_2/CNT(c-d) and PEDOT/CNT(e-f).

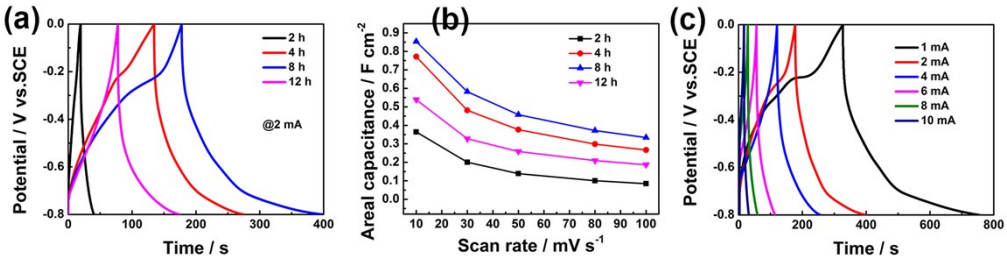

Figure S9. Electrochemical properties comparison for different SnS_2/CNT-x electrodes: (a) CV curves at 30 mV s^{-1}, (b) GCD curves at 2 mA. (c) Capacitance of the SnS_2/CNT-x electrodes at different scan rates. (d) Nyquist plots of the SnS_2/CNT-x electrodes. Electrochemical properties of the SnS_2/CNT-8 electrode: (e) CV curves, (f) GCD curves at different currents.

The SnS_2/CNT-8 electrode demonstrated much higher electrochemical properties than other SnS_2/CNT-x electrodes, including longer discharge time at 2 mA (Figure S9a). The introduction of flexible, electrically conductive CNT film substrate gives strong support for the SnS_2 nanosheets to provide a short ion diffusion path, and prevents their agglomeration and fast fading in capacity, thereby maintaining structural integrity during the electrochemical process and significantly improving the reversible capacity of the SnS_2/CNT electrode. The 2D SnS_2/CNT-8 structure with high surface area and nanocrystalline wall structure plays a key role in providing rapid electrolyte transport and shorter diffusion paths, as well as provides more active sites for electrochemical reactions. The specific capacitances calculated from the CV curves at various scan rates are shown in Figure S9b, where the capacitance improved significantly as the reaction time increased from 2 to 8 h. Further increasing the reaction time resulted in thicker SnS_2 layers that limit the accessible inner surface area for electrochemical charge storage, which offsets the contribution of the increased SnS_2 active materials and leads to a lower areal capacitance. The cyclic voltammetry (CV) and galvanostatic charge-discharge (GCD) curves of the SnS_2/CNT-8 electrode exhibited excellent pseudo-capacitance properties in the potential range of -0.8~0 V (Figure S9c).

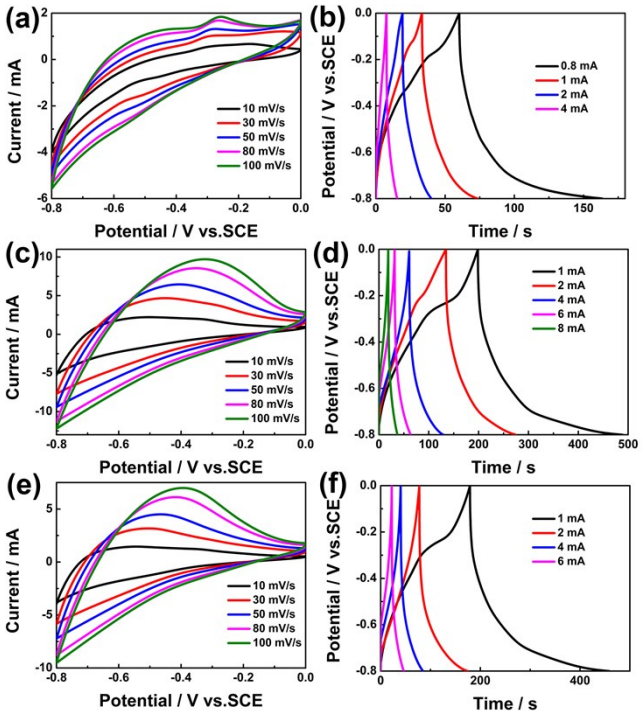

Figure S10. Electrochemical properties of the SnS_2/CNT: (a-b) SnS_2/CNT-2; (e-f)SnS_2/CNT-4; (g-h) SnS_2/CNT-12.

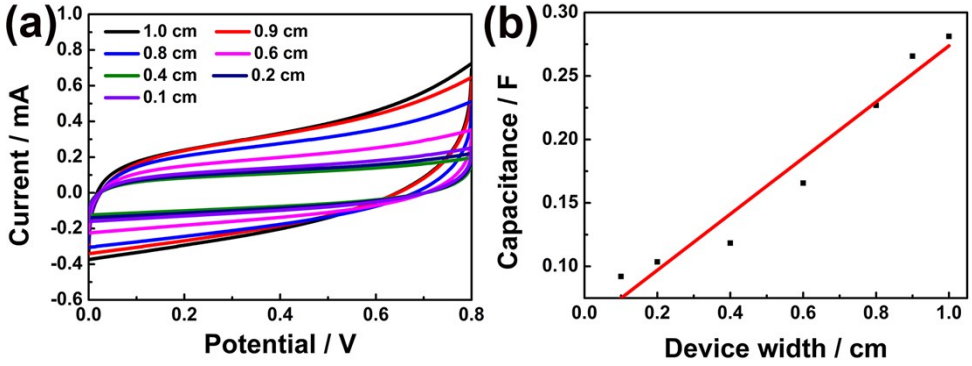

Figure S11. (a)CV curves of the different device width, (b) Linear relationship between the capacitance and device width.

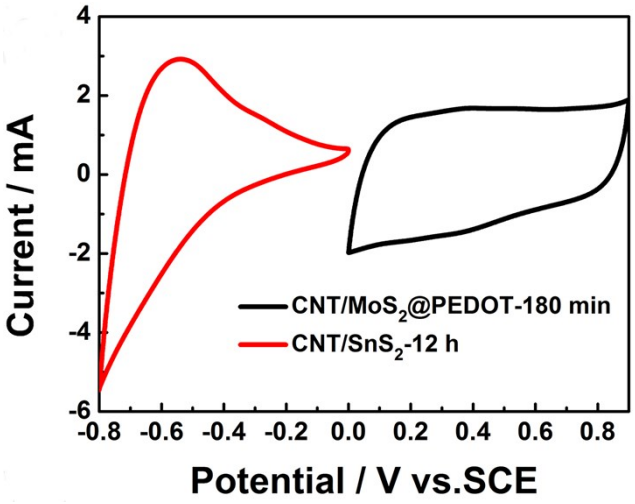

Figure S12. CV curves of SnS_2/CNT-12 and MoS_2/PEDOT/CNT-180 electrodes obtained in a three-electrode system in 3 M LiCl aqueous solution at the scan rate of 30 mV s^{-1}.

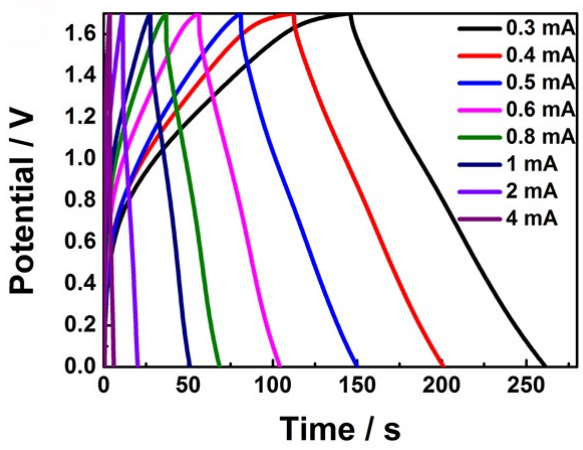

Figure S13. GCD curves of sheet type ASC.

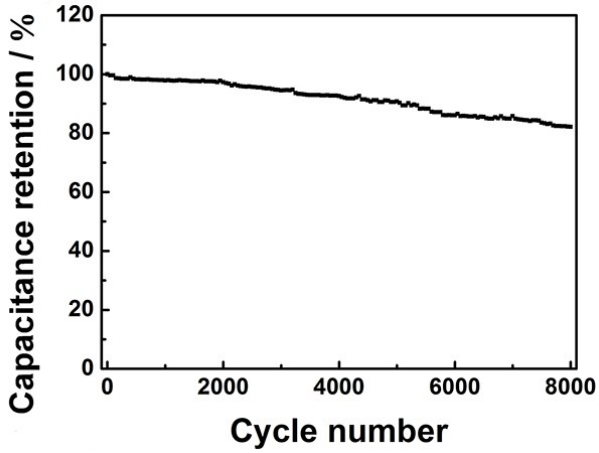

Figure S14. Cycling performance of the sheet type ASC device

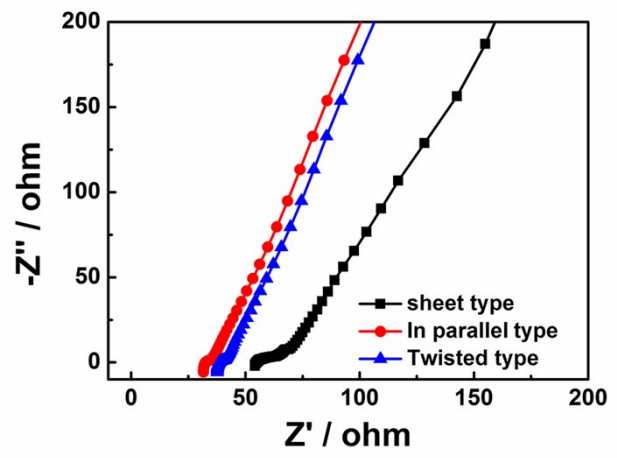

Figure S15. EIS curve of three types devices.

Figure S16. Digital image of the packaged device in water.